

Synthesis and iron binding studies of *myo*-inositol 1,2,3-trisphosphate and (\pm)-*myo*-inositol 1,2-bisphosphate, and iron binding studies of all *myo*-inositol tetrakisphosphates ¹

Ian D. Spiers ^a, Christopher J. Barker ^b, Sung-Kee Chung ^c,
Young-Tae Chang ^c, Sally Freeman ^{a,d,*}, John M. Gardiner ^e,
Peter H. Hirst ^f, Peter A. Lambert ^a, Robert H. Michell ^b,
David R. Poyner ^a, Carl H. Schwalbe ^a, Anthony W. Smith ^f,
Kevin R.H. Solomons ^d

^a Department of Pharmaceutical and Biological Sciences, Aston University, Aston Triangle, Birmingham B4 7ET, UK

^b Centre for Clinical Research in Immunology and Signalling, Birmingham University, Birmingham B15 2TT, UK

^c Department of Chemistry, Pohang University of Science and Technology, Pohang 790-784, South Korea

^d Department of Pharmacy, University of Manchester, Oxford Road, Manchester M13 9PL, UK

^e Department of Chemistry, University of Manchester Institute of Technology (UMIST), P.O. Box 88, Manchester M60 1QD, UK

^f School of Pharmacy and Pharmacology, University of Bath, Claverton Down, Bath BA2 7AY, UK

Received 23 May 1995; accepted 21 September 1995

Abstract

The first syntheses of the natural products *myo*-inositol 1,2,3-trisphosphate and (\pm)-*myo*-inositol 1,2-bisphosphate are described. The protected key intermediates 4,5,6-tri-*O*-benzoyl-*myo*-inositol and (\pm)-3,4,5,6-tetra-*O*-benzyl-*myo*-inositol were phosphorylated with dibenzyl *N,N*-diisopropylphosphoramidite in the presence of 1*H*-tetrazole and subsequent oxidation of the phosphite. The crystal structures of the synthetic intermediates (\pm)-1-*O*-(*tert*-butyldiphenylsilyl)-2,3-*O*-cyclohexylidene-*myo*-inositol and (\pm)-4,5,6-tri-*O*-benzoyl-1-*O*-(*tert*-butyldiphenylsilyl)-

* Corresponding author. For correspondence regarding the chemistry and reprint requests contact S. Freeman at the University of Manchester. For iron binding studies contact D.R. Poyner.

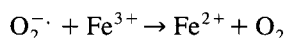
¹ A preliminary account of part of this study has been published in ref. [1].

2,3-*O*-cyclohexylidene-*myo*-inositol are reported. *myo*-Inositol 1,2,3-trisphosphate, (\pm)-*myo*-inositol 1,2-bisphosphate, and all isomeric *myo*-inositol tetrakisphosphates were evaluated for their ability to alter HO \cdot production in the iron-catalysed Haber–Weiss reaction. The results demonstrated that a 1,2,3-grouping of phosphates in *myo*-inositol was necessary for inhibition, also that (\pm)-*myo*-inositol 1,2-bisphosphate potentiated HO \cdot production. *myo*-Inositol 1,2,3-trisphosphate resembled *myo*-inositol hexakisphosphate (phytic acid) in its ability to act as a siderophore by promoting iron-uptake into *Pseudomonas aeruginosa*.

Keywords: *myo*-Inositol 1,2,3-trisphosphate; (\pm)-*myo*-Inositol 1,2-bisphosphate; *myo*-Inositol tetrakisphosphates; Antioxidant; Siderophore

1. Introduction

myo-Inositol hexakisphosphate (InsP $_6$, phytic acid) is the most abundant organic form of phosphate, found in all eucaryotic cells, and also in soil [2]. It has potential in the prevention and treatment of a range of cancers [3], however, its biological role remains uncertain [4]. InsP $_6$ may simply be a phosphate or inositol store, being metabolised to other inositol phosphates or pyrophosphates [5]. Alternatively, it may be a neurotransmitter [6], though the effects may be caused by its chelation with calcium [7]. Another possible function arises from its antioxidant and metal chelation properties [8]. InsP $_6$ is of interest to nutritionists, as it can prevent absorption of trace metals. Graf and co-workers [9] showed that chelation of Fe $^{3+}$ to InsP $_6$ prevented formation of the highly reactive hydroxyl radical (HO \cdot) from the superoxide radical anion (O $_2^{\cdot-}$) by the iron-catalysed Haber–Weiss redox cycle [10]:



These results suggest that the Fenton reaction does not occur with the InsP $_6$ –iron chelate, and this has been attributed to the unavailability of a coordination site for H $_2$ O $_2$ in the complex [9]. They also proposed that the oxidation of Fe $^{2+}$ by molecular oxygen (reverse of first step) was catalysed by InsP $_6$ and that this contributes to the antioxidant properties of InsP $_6$ [11]. In contrast, Burkitt and Gilbert concluded that phytic acid catalyses the Fenton reaction, but blocks the first step of the Haber–Weiss cycle [12,13]. Some iron chelates, for example with ADP, do catalyse the formation of hydroxy radicals [14], which was attributed to the increased solubility of iron on complexation and to the availability of a readily dissociable water ligand [9].

InsP $_6$ is an excellent chelator of Fe $^{3+}$ (K 10 25 –10 30) [15], and it has been proposed that InsP $_6$ may be an intracellular, low molecular weight chelator of Fe $^{3+}$ [16]. In addition, we have described how InsP $_6$ can be used as a siderophore by *Pseudomonas aeruginosa*, suggesting that InsP $_6$ may have a role in supplying Fe $^{3+}$ to free-living organisms [17].

InsP $_6$, either in the crystalline form as the dodecasodium salt or bound to deoxy-hemoglobin, adopts a chair conformation, with five of the phosphate groups (1-, 3-, 4-, 5-, and 6-) in axial positions [18,19]. NMR studies support this conclusion, but suggest

that these five phosphate groups adopt equatorial positions in solution as the free acid form, with the conformational change occurring at pH 9.4 [20]. Of relevance, Evans and Martin have studied the interactions of Fe^{3+} and Al^{3+} with InsP_6 by calorimetry [21,22]: Insoluble complexes were formed which contained 4 equivalents of metal cation for each InsP_6 .

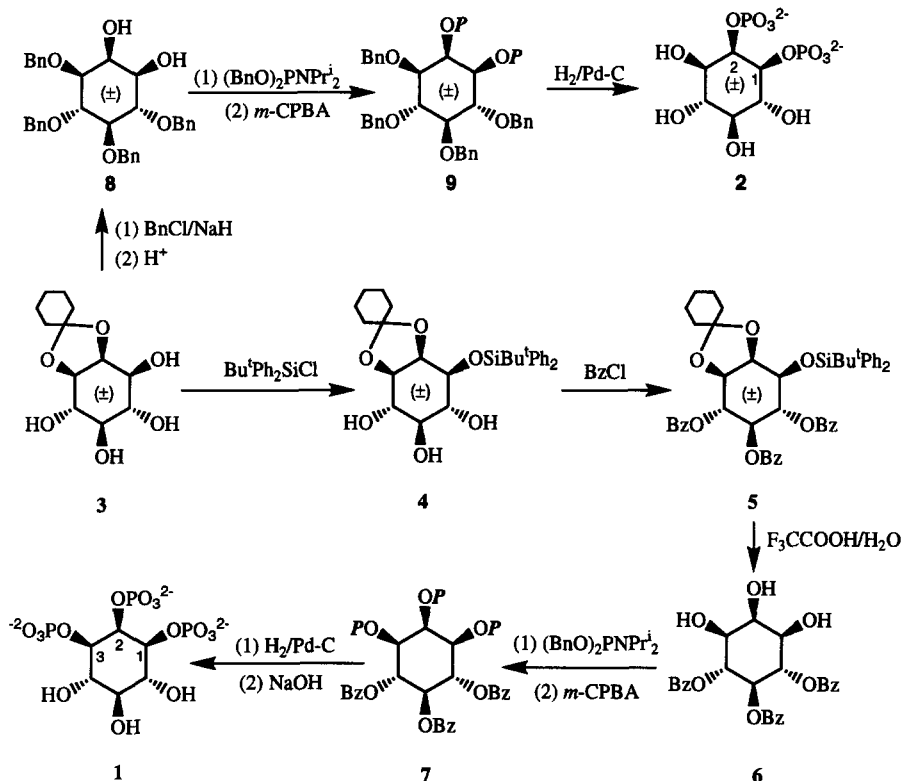
Further understanding of the iron-binding properties of InsP_6 has come from examination of inositol pentakisphosphate isomers which all bind Fe^{3+} with high affinity. However, only those possessing a *cis*-(1,2,3)(equatorial–axial–equatorial)-trisphosphate grouping are also antioxidant, completely inhibiting hydroxyl radical formation [16]. Of considerable significance to this study, *myo*-inositol 1,2,3-trisphosphate [**1**, $\text{Ins}(1,2,3)\text{P}_3$] has recently been reported to be present in mammalian cells at concentrations of 1–10 μM [23–25]. Barker and co-workers [24,25] proposed that this compound may have a role in iron chelation in the cell.

To test this proposal, we here report the preparation of **1**, hitherto only available in small quantities from biochemical sources. The synthesis of the recently isolated cell constituent (\pm)-*myo*-inositol 1,2-bisphosphate [**2**, (\pm)- $\text{Ins}(1,2)\text{P}_2$] is also presented; this has apparently not been reported before [26]. The antioxidant properties of these natural products and of all the *myo*-inositol tetrakisphosphates [27] are described here, along with the ability of $\text{Ins}(1,2,3)\text{P}_3$ to facilitate iron uptake into *Pseudomonas aeruginosa*.

2. Results and discussion

Synthesis and X-ray crystallography.—The synthesis of $\text{Ins}(1,2,3)\text{P}_3$ (**1**) was completed as shown in Scheme 1. Tetrol **3** was prepared from the reaction of *myo*-inositol and 1,1-diethoxycyclohexane to give a mixture of bisacetals [28], with subsequent removal of the *trans*-cyclohexylidene ring [29]. Utilising the procedure developed by Bruzik and Tsai [30], tetrol **3** was regioselectively silylated at position 1 in 58% yield. The structure of product **4** was elucidated by X-ray crystallography (see below). Compound **4** was treated with benzoyl chloride to give the tribenzoate **5** in 73% yield, the structure of which was also confirmed by X-ray crystallography (see below). Both the *cis*-cyclohexylidene and silyl groups of **5** were removed in one step by treatment with aqueous trifluoroacetic acid at 50 °C to give 4,5,6-tri-*O*-benzoyl-*myo*-inositol (**6**), which was crystallised from diethyl ether. Compound **6** was the only product isolated from the reaction, and it is possible that some hydrolysis or migration of the benzoyl groups could account for the low (49%) yield [31]. The triol **6** was treated with dibenzyl *N,N*-diisopropylphosphoramidite [32] and the phosphite intermediate was oxidised with 3-chloroperoxybenzoic acid to give 4,5,6-tri-*O*-benzoyl-*myo*-inositol 1,2,3-tris(dibenzyl phosphate) (**7**) in 56% yield. Deprotection of **7** was achieved (82%) by hydrogenolysis followed by base-catalysed hydrolysis of the benzoyl esters to give $\text{Ins}(1,2,3)\text{P}_3$ (**1**), which crystallised as its monosodium tetra(cyclohexylammonium) salt. The crystal structure has recently been described, which exists in a chair conformation with five substituents equatorial and one axial [33].

The crystal structures of intermediates **4** and **5** were solved by X-ray crystallography



Scheme 1. Synthesis of *myo*-inositol 1,2,3-trisphosphate (**1**) and (\pm) -*myo*-inositol 1,2-bisphosphate (**2**). $P = (\text{BnO})_2\text{P(O)}^-$.

(Table 1)². All the *myo*-inositol compounds have the expected chair conformation with 1-ax/5-eq oxygen positions, in contrast to phytate with its unusual 1-eq/5-ax conformation [18,19]. The inositol ring bond distances and angles for the two structures are consistent with one another and with those of *myo*-inositol itself [35].

Two molecules of triol **4** were found to crystallise with one molecule of DMF and one molecule of chloroform with half occupancy (Figs. 1 and 2, and Table 2) in each asymmetric unit. The inositol rings of the two molecules are different in that one ring is twisted with a good two-fold axis retained $\Delta C_2(\text{C}2-\text{C}3) = 2.28$ and the other ring is flattened at one end (C75) and puckered at the opposite end (C78), retaining a good mirror plane $\Delta C_s(\text{C}75) = 2.85$ (asymmetry parameters, [37]). These differences in ring puckering for the same chemical structure show how crystal packing and hydrogen bonding play an important part in determining the conformation of flexible rings and

² Complete tables of temperature factors, hydrogen atom coordinates, and bond lengths and angles have been deposited at the Cambridge Crystallographic Data Centre. These data may be obtained on request, from the Director, Cambridge Crystallographic Data Centre, 12 Union Road, Cambridge CB2 1E2, UK.

Table 1

Crystal data for (\pm)-1-*O*-(*tert*-butyldiphenylsilyl)-2,3-*O*-cyclohexylidene-*myo*-inositol (**4**) and (\pm)-4,5,6-tri-*O*-benzoyl-1-*O*-(*tert*-butyldiphenylsilyl)-2,3-*O*-cyclohexylidene-*myo*-inositol (**5**)

	4	5
Formula (per asymmetric unit)	$2 \times \text{C}_{28}\text{H}_{38}\text{O}_6\text{Si}$ + $\text{C}_3\text{H}_7\text{NO}$ (DMF) + $1/2 \times \text{CHCl}_3$	$\text{C}_{49}\text{H}_{50}\text{O}_9\text{Si}$
Crystal size (mm)	$0.35 \times 0.25 \times 0.10$	$0.40 \times 0.25 \times 0.05$
Crystal system	Triclinic	Monoclinic
Space group	$P\bar{1}$	Pn
Cell dimensions		
a (Å)	9.556(3)	14.358(4)
b (Å)	16.834(3)	11.448(5)
c (Å)	20.186(4)	14.603(6)
α (°)	80.45(2)	90
β (°)	77.74(2)	111.60(3)
γ (°)	89.02(2)	90
V (Å ³)	3129(1)	2232(2)
Z	2	2
D_{calcd} (g cm ⁻³)	1.200	1.207
$F(000)/e$	1210	860
Total no. of reflections	9744	4994
No. of observed reflections	4463	2440
Absorption coefficient (mm ⁻¹)	0.180	0.107
Final residuals		
$R[F]^a$	0.0604	0.0475
$R_w[F^2]^a$	0.1596	0.1171
Largest difference peak (e Å ⁻³)	0.394	0.157
Largest difference hole (e Å ⁻³)	-0.244	-0.195
Absolute structure parameter [34]	N/A ^b	0.21(29)

^a R factors are tabulated for observed reflections satisfying the criterion $> 4\sigma(F_o)$.

^b Not applicable.

that care must be taken when trying to extrapolate precise structural detail from crystal structures. The three OH groups of both inositol molecules are involved in donating hydrogen bonds (Table 3, the values are in good agreement with surveyed data [38]). Two OH groups in each molecule also accept hydrogen bonds. O10 and O83 (OH groups at position C-4 in the two triol molecules) are involved in homodromic hydrogen bonding [39] with symmetry-related molecules forming a tetramer.

The inositol ring of **5** (Fig. 3 and Table 4) is also flattened at one end (C2) and puckered at the opposite end (C5), with a good mirror plane retained $\Delta C_s(C2) = 2.28$ [37]. The carbonyl bonds on the benzoyl groups point in the same direction as the C–H bonds on the inositol ring and are approximately coplanar with their corresponding inositol C–O bonds (C–O–C–O torsion angles range from 3.2 to 6.3°) which is also seen in the crystal structure of 1,2,3,4,5,6-hexa-*O*-acetyl-*myo*-inositol [40]. This *s-trans* conformation is best explained by a secondary electronic effect where the ether oxygen has an electron pair which is oriented antiperiplanar to the C–O σ bond of the carbonyl

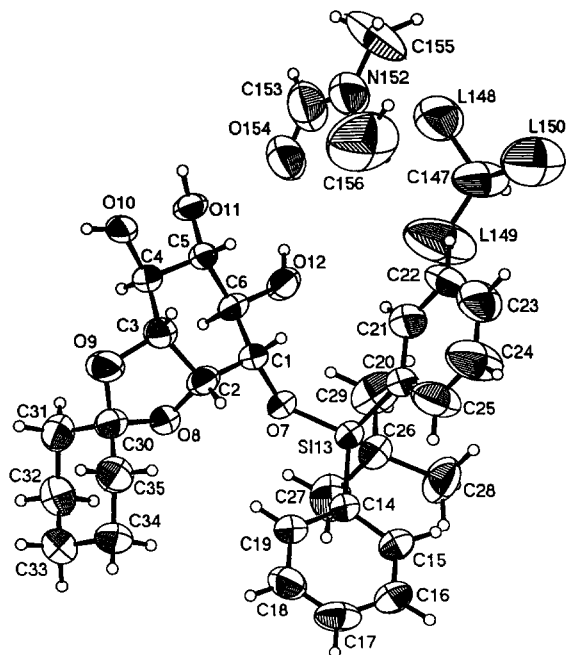


Fig. 1. ORTEP drawing [36] of "molecule one" of (\pm) -1-*O*-(*tert*-butyldiphenylsilyl)-2,3-*O*-cyclohexylidene-*myo*-inositol (**4**) with DMF and the CHCl_3 , site showing the labelling scheme for non-H atoms (L=Cl). Thermal ellipsoids are drawn at the 50% probability level.

group. This electron pair orbital can therefore overlap with the antibonding orbital σ^* of that bond and is suggested to result in a ca. 3 kcal/mol increase in stability [41].

The synthesis of (\pm) -Ins(1,2) P_2 was completed as shown in Scheme 1. Using the procedure developed by Baker and co-workers [29], (\pm) -tetra-*O*-benzyl-*myo*-inositol (**8**) was prepared from tetrol **3** by benzylation with benzyl chloride–NaH followed by acid-catalysed removal of the acetal group. Diol **8** was phosphorylated using dibenzyl *N,N*-diisopropylphosphoramidite and 3-chloroperoxybenzoic acid [32] to give (\pm) -3,4,5,6-tetra-*O*-benzyl-*myo*-inositol 1,2-bis(dibenzyl phosphate) (**9**) in 98% yield. The benzyl groups of **9** could be removed by hydrogenolysis in ethanol, but the presence of peaks between δ_{H} 1.2–1.0 and δ_{H} 3.9–3.4 in the ^1H NMR spectrum suggested that hydrogenolysis may be accompanied by a small amount of ethanolysis. However, when the solvent was changed to THF–water, hydrogenolysis of **9** in the presence of Pd–C catalyst cleanly removed the benzyl substituents. The free acid of **2** was passed down a Dowex-50 cation-exchange column (sodium form) to give trisodium (\pm) -*myo*-inositol 1,2-bisphosphate in 87% yield. For the syntheses of both **1** and **2**, all new compounds were fully characterised by ^1H , ^{13}C , and ^{31}P NMR spectroscopy, IR and mass spectrometry, and elemental analysis.

Antioxidant function.—The abilities of Ins(1,2,3) P_3 (**1**), (\pm) -Ins(1,2) P_2 (**2**), and all the regioisomeric *myo*-inositol tetrakisphosphates to alter Fe^{3+} -catalysed HO^\cdot formation were assessed. Hydroxyl radical was generated and measured in the following assay: in

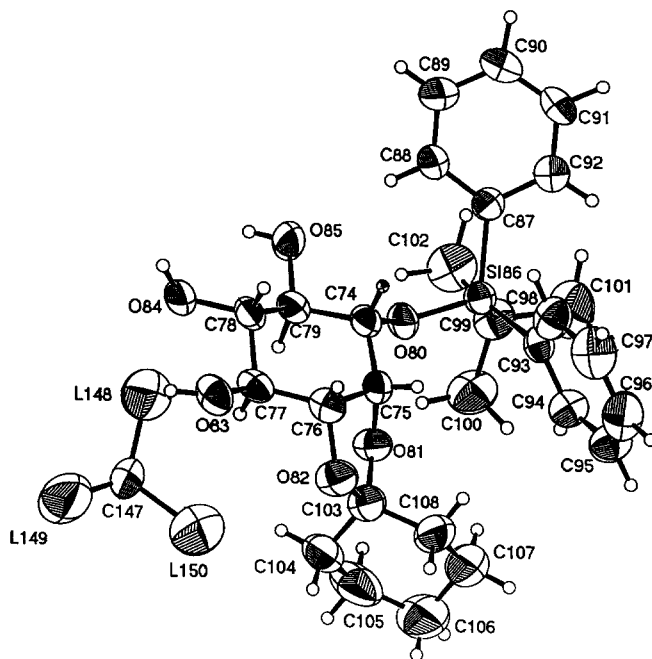
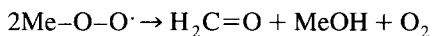


Fig. 2. ORTEP drawing [36] of “molecule two” of (\pm) -1-*O*-(*tert*-butyldiphenylsilyl)-2,3-*O*-cyclohexylidene-*myo*-inositol (**4**) with the CHCl_3 site (also included as a reference point), showing the labelling scheme for non-H atoms (L=Cl). Thermal ellipsoids are drawn at the 50% probability level.

the presence of xanthine oxidase, hypoxanthine was oxidised by molecular oxygen to give xanthine, the superoxide radical anion O_2^- ; and hydrogen peroxide. The latter two products participated in the iron-catalysed Haber–Weiss process to give $\text{HO}\cdot$; which reacted with dimethyl sulfoxide (present in the assay). The first intermediate formed was the methyl radical, which reacts by at least three routes [42]: it can abstract a hydrogen to give methane, dimerise to give ethane, or react with molecular oxygen to give $\text{Me-O-O}\cdot$; and thence formaldehyde:



The ability of the inositol phosphates to chelate with iron and inhibit or catalyse $\text{HO}\cdot$ formation was evaluated by assaying the formaldehyde released by the Hantzsch reaction [43]. This required incubation of the reaction mixture with pentane-2,4-dione at 60°C , with subsequent measurement of absorbance at 410 nm.

Both $\text{Ins}(1,2,3)\text{P}_3$ and InsP_6 completely inhibited Fe^{3+} -catalysed hydroxyl radical formation at $> 100 \mu\text{M}$ (Table 5), in support of the earlier hypothesis that the *cis*-1,2,3(equatorial–axial–equatorial)-triphosphate grouping in InsP_6 is needed to inhibit Fe^{3+} -catalysed hydroxyl radical formation. It is also possible that this allows InsP_6 and $\text{Ins}(1,2,3)\text{P}_3$ to function as “safe” carriers of Fe^{3+} within the cell.

Further confirmation that the 1,2,3-triphosphate grouping is required for inhibition of Fe^{3+} -catalysed $\text{HO}\cdot$ formation came from studying the family of *myo*-inositol tetra-

Table 2

Atomic coordinates ($\times 10^4$) and equivalent isotropic displacement parameters ($\text{\AA}^2 \times 10^3$) for (\pm)-1-*O*-(*tert*-butyldiphenylsilyl)-2,3-*O*-cyclohexylidene-*myo*-inositol (**4**)^a

Atom	<i>x</i>	<i>y</i>	<i>z</i>	<i>U</i> _{eq}
C1	3250(5)	3288(3)	2964(2)	50(1)
C2	1891(6)	3687(3)	2819(2)	54(1)
C3	1096(6)	4162(3)	3361(2)	58(1)
C4	2042(6)	4594(3)	3708(2)	56(1)
C5	3251(5)	4076(3)	3890(2)	47(1)
C6	4154(5)	3812(3)	3255(2)	49(1)
O7	4063(3)	3028(2)	2366(1)	52(1)
O8	2145(3)	4275(2)	2210(1)	54(1)
O9	340(4)	4752(2)	2969(2)	78(1)
O10	1240(5)	4810(2)	4329(2)	78(1)
O11	4163(4)	4496(2)	4197(2)	57(1)
O12	5358(4)	3372(2)	3416(2)	67(1)
Si13	4412(2)	2115(1)	2190(1)	51(1)
C14	3197(5)	1866(3)	1638(2)	53(1)
C15	3241(6)	1127(3)	1399(2)	70(2)
C16	2358(7)	939(3)	999(3)	80(2)
C17	1386(7)	1491(4)	809(3)	78(2)
C18	1300(6)	2219(3)	1032(2)	71(2)
C19	2201(5)	2402(3)	1437(2)	58(1)
C20	4080(6)	1350(3)	2993(2)	63(1)
C21	4700(6)	1439(3)	3548(3)	76(2)
C22	4451(8)	879(4)	4151(3)	93(2)
C23	3607(9)	223(4)	4210(3)	116(3)
C24	3001(10)	116(4)	3674(4)	137(3)
C25	3223(8)	669(3)	3088(3)	106(2)
C26	6336(6)	2174(3)	1692(2)	65(1)
C27	6447(8)	2798(4)	1034(3)	99(2)
C28	6840(7)	1355(3)	1494(3)	93(2)
C29	7332(6)	2430(4)	2126(3)	94(2)
C30	895(6)	4757(3)	2254(2)	62(1)
C31	1350(6)	5598(3)	1889(3)	75(2)
C32	1767(7)	5650(3)	1121(3)	88(2)
C33	587(8)	5335(3)	827(3)	92(2)
C34	176(7)	4485(3)	1174(3)	80(2)
C35	−242(6)	4417(3)	1945(3)	76(2)
C74	2669(5)	3216(2)	7250(2)	45(1)
C75	1500(5)	2663(2)	7168(2)	44(1)
C76	597(5)	2984(3)	6651(2)	49(1)
C77	1418(5)	3504(2)	6010(2)	46(1)
C78	2368(6)	4122(3)	6178(2)	48(1)
C79	3425(5)	3700(3)	6577(2)	50(1)
O80	3684(3)	2768(2)	7576(1)	46(1)
O81	2109(3)	1973(2)	6904(2)	53(1)
O82	61(4)	2260(2)	6502(2)	64(1)
O83	412(4)	3869(2)	5625(2)	59(1)
O84	3110(4)	4594(2)	5568(2)	61(1)
O85	4357(4)	4251(2)	6733(2)	76(1)
Si86	3645(1)	2496(1)	8398(1)	46(1)

Table 2 (continued)

Atom	x	y	z	U_{eq}
C87	3746(5)	3415(2)	8797(2)	49(1)
C88	4130(6)	4160(3)	8407(2)	59(1)
C89	4214(6)	4838(3)	8700(3)	71(2)
C90	3938(6)	4772(3)	9403(3)	77(2)
C91	3582(6)	4037(3)	9803(2)	75(2)
C92	3478(6)	3372(3)	9508(2)	69(2)
C93	1915(5)	1951(3)	8844(2)	49(1)
C94	1720(6)	1122(3)	8901(2)	66(1)
C95	411(8)	749(4)	9205(3)	79(2)
C96	-727(7)	1174(4)	9444(3)	79(2)
C97	-595(7)	1998(4)	9395(3)	79(2)
C98	720(6)	2371(3)	9099(2)	62(1)
C99	5273(6)	1860(3)	8411(3)	64(1)
C100	5378(7)	1218(3)	7944(3)	85(2)
C101	5319(7)	1457(4)	9155(3)	97(2)
C102	6606(6)	2429(3)	8145(3)	84(2)
C103	988(5)	1610(3)	6677(2)	57(1)
C104	1630(7)	1249(3)	6057(3)	78(2)
C105	2523(9)	529(4)	6241(3)	111(2)
C106	1644(9)	-99(3)	6799(4)	128(3)
C107	1023(8)	266(3)	7420(3)	96(2)
C108	135(6)	992(3)	7248(3)	75(2)
C147	9957(19)	1707(7)	4233(6)	122(6)
L148	10291(5)	2399(2)	4696(2)	123(1)
L149	9195(7)	2056(3)	3590(3)	200(3)
L150	9309(7)	829(3)	4724(2)	167(2)
N152	6637(7)	2838(3)	5430(3)	103(2)
C153	7154(8)	3543(4)	5054(4)	112(2)
O154	7077(6)	3804(2)	4441(3)	116(2)
C155	6902(10)	2554(6)	6087(4)	153(3)
C156	5648(15)	2401(6)	5155(6)	213(5)

^a "Molecule one" has atoms C1 to C35 and "molecule two" has atoms C74 to C108. L refers to the chlorine atoms of CHCl_3 . U_{eq} is defined as one-third of the trace of the orthogonalised U_{ij} tensor.

kisphosphates. Only $\text{Ins}(1,2,3,5)\text{P}_4$ and $(\pm)\text{-Ins}(1,2,3,4)\text{P}_4$ were able completely, or almost completely, to inhibit HO^\cdot generation when present at 100 μM , thereby resembling InsP_6 (Table 5). As expected, $(\pm)\text{-Ins}(1,2)\text{P}_2$ failed to inhibit HO^\cdot produc-

Table 3

Hydrogen bonding in $(\pm)\text{-1-O-(tert-butyl)diphenylsilyl)-2,3-O-cyclohexylidene-myio-inositol}$ (**4**)

	$d_{\text{O} \cdots \text{O}}$ (Å)	$d_{\text{O-H} \cdots \text{O}}$ (Å)	$\alpha_{\text{O-H} \cdots \text{O}}$ (°)	Symmetry acceptor
O10–H10 \cdots O83	2.707(5)	1.88(6)	170(5)	(-x, 1-y, 1-z)
O11–H11 \cdots O84	2.767(4)	1.73(8)	156(7)	(x, y, z)
O12–H12 \cdots O154	3.082(6)	2.24(6)	170(6)	(x, y, z)
O83–H83 \cdots O10	2.788(5)	1.97(5)	171(5)	(x, y, z)
O84–H84 \cdots O154	2.696(5)	1.90(5)	172(6)	(1-x, 1-y, 1-z)
O85–H85 \cdots O11	2.763(5)	2.01(5)	157(4)	(1-x, 1-y, 1-z)

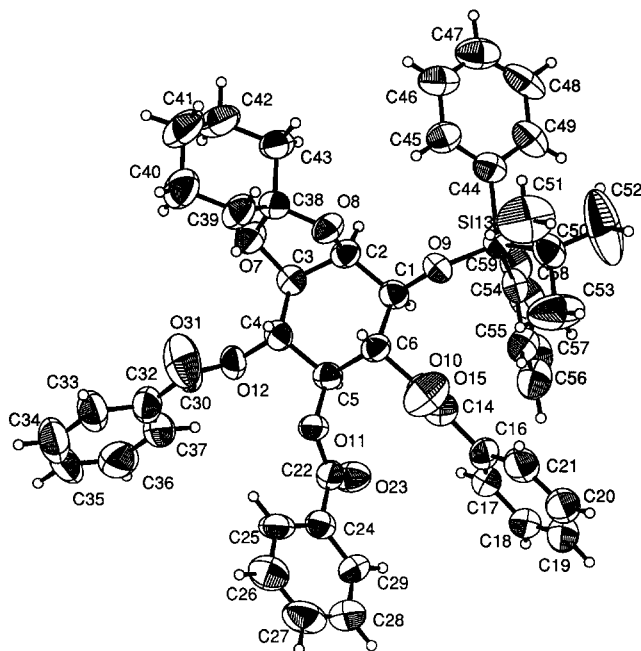


Fig. 3. ORTEP drawing [36] of (\pm) -4,5,6-tri-*O*-benzoyl-1-*O*-(*tert*-butyldiphenylsilyl)-2,3-*O*-cyclohexylidene-*myo*-inositol (**5**) showing the labelling scheme for non-H atoms. Thermal ellipsoids are drawn at the 50% probability level.

tion. Unexpectedly, however, it substantially potentiated free radical production, thereby resembling other iron chelators such as ATP or EDTA [9,12,44]. An Fe^{3+} – (\pm) -Ins(1,2) P_2 complex may have less steric constraints than Fe^{3+} –Ins(1,2,3) P_3 , so perhaps this allows H_2O or H_2O_2 to enter the co-ordination sphere in the former complex: Graf and co-workers [9] have suggested that this would enhance $\text{HO}\cdot$ production. However, the difference in properties may also be attributed to a change in redox-potential between the complexes [13,14].

Interestingly, it has recently been reported that Ins(1,2,6) P_3 , Ins(1,3,5) P_3 , and Ins(2,4,6) P_3 each give a range of strong complexes with Fe^{3+} [45]. The derivative with three vicinal phosphates, Ins(1,2,6) P_3 (equatorial–equatorial–axial), binds Fe^{3+} more strongly than the three alternated phosphates of either Ins(1,3,5) P_3 or Ins(2,4,6) P_3 . It was proposed that with Ins(1,2,6) P_3 the arrangement of the phosphates is such that they all participate in binding with Fe^{3+} [45]. In contrast, for Ins(2,4,6) P_3 , the axial phosphate on position 2 largely contributes to complex stabilisation.

It is clear that different Fe^{3+} –inositol phosphate complexes can show a range of properties and further studies are underway to determine the stoichiometry of the species present in our experiments. Further studies with Ins P_3 and Ins P_2 isomers are now needed to see whether some simple structural motif can explain the enhanced $\text{HO}\cdot$ generation seen with (\pm) -Ins(1,2) P_2 , in contrast to inhibition of this phenomenon by the 1,2,3-trisphosphate grouping. The possible biological consequences of enhanced $\text{HO}\cdot$ generation

Table 4

Atomic coordinates ($\times 10^4$) and equivalent isotropic displacement parameters ($\text{\AA}^2 \times 10^3$) for (\pm)-4,5,6-tri-*O*-benzoyl-1-*O*-(*tert*-butyldiphenylsilyl)-2,3-*O*-cyclohexylidene-*myo*-inositol (**5**)

Atom	<i>x</i>	<i>y</i>	<i>z</i>	U_{eq}^a
C1	1309(5)	2848(7)	10198(6)	52(2)
C2	373(5)	3610(7)	9868(6)	51(2)
C3	-620(5)	2967(8)	9640(6)	50(2)
C4	-551(6)	2032(7)	10412(6)	50(2)
C5	333(6)	1231(7)	10556(6)	48(2)
C6	1291(6)	1954(7)	10955(6)	50(2)
O7	-1274(3)	3887(5)	9695(4)	60(2)
O8	357(4)	4393(5)	10615(4)	57(1)
O9	2187(3)	3541(5)	10594(3)	51(1)
O10	2103(3)	1157(5)	11104(3)	50(1)
O11	361(4)	356(5)	11268(4)	54(1)
O12	-1455(4)	1336(5)	10039(4)	57(2)
Si13	2984(1)	3892(2)	10057(2)	51(1)
C14	2765(6)	997(9)	12005(6)	63(2)
O15	2795(5)	1536(7)	12715(5)	98(2)
C16	3504(5)	51(9)	12030(6)	59(2)
C17	3279(6)	-780(8)	11332(7)	63(2)
C18	3946(7)	-1678(9)	11374(8)	81(3)
C19	4867(8)	-1668(11)	12138(10)	100(4)
C20	5132(7)	-821(11)	12846(9)	89(3)
C21	4423(6)	57(10)	12815(7)	82(3)
C22	562(5)	-744(8)	11058(7)	54(2)
O23	633(4)	-1022(5)	10294(4)	71(2)
C24	710(5)	-1569(8)	11888(6)	54(2)
C25	224(6)	-1406(7)	12553(6)	67(2)
C26	366(8)	-2178(10)	13299(8)	85(3)
C27	1006(9)	-3099(11)	13409(8)	95(3)
C28	1492(8)	-3256(10)	12766(10)	100(4)
C29	1318(6)	-2487(8)	12002(8)	73(3)
C30	-1995(6)	1279(9)	10613(7)	64(2)
O31	-1822(5)	1779(8)	11354(6)	110(3)
C32	-2850(6)	477(10)	10179(7)	73(3)
C33	-3612(7)	464(11)	10579(8)	89(3)
C34	-4384(8)	-282(16)	10226(11)	116(5)
C35	-4472(8)	-1036(13)	9468(13)	118(5)
C36	-3752(8)	-1067(10)	9056(10)	111(4)
C37	-2926(6)	-299(9)	9432(8)	81(3)
C38	-652(6)	4796(7)	10328(6)	55(2)
C39	-916(6)	4934(9)	11233(6)	71(3)
C40	-1982(8)	5336(10)	10958(8)	92(3)
C41	-2164(9)	6461(10)	10382(9)	105(4)
C42	-1906(8)	6332(9)	9478(8)	95(3)
C43	-827(6)	5916(8)	9744(7)	69(2)
C44	2614(6)	5330(8)	9409(6)	60(2)
C45	1923(6)	6048(8)	9613(6)	63(2)
C46	1675(8)	7141(9)	9189(8)	80(3)
C47	2091(9)	7537(9)	8558(8)	85(3)
C48	2780(8)	6859(11)	8336(7)	84(3)

Table 4 (continued)

Atom	x	y	z	U_{eq}
C49	3044(7)	5751(9)	8763(6)	77(3)
C50	4238(6)	4078(9)	11089(6)	69(2)
C51	4112(10)	4975(12)	11800(8)	136(5)
C52	5019(8)	4473(18)	10729(10)	191(9)
C53	4574(9)	2961(10)	11689(10)	151(7)
C54	2940(6)	2712(8)	9147(6)	56(2)
C55	3207(6)	1551(8)	9483(7)	64(2)
C56	3158(6)	646(10)	8863(8)	79(3)
C57	2821(7)	842(11)	7898(8)	79(3)
C58	2522(7)	1933(11)	7513(7)	81(3)
C59	2576(6)	2853(9)	8143(7)	69(2)

^a U_{eq} is defined as one-third of the trace of the orthogonalised U_{ij} tensor.

by some inositol phosphates and inhibition by others is intriguing. Ins(1,2,3)P₃ when present with (±)-Ins(1,2)P₂ at equimolar concentrations can still totally suppress HO· generation [46]; it will be of interest to determine how it can interact with other inositol phosphates or biologically relevant Fe³⁺ chelators such as ATP.

Siderophore activity.—We have previously described how InsP₆ can act as a siderophore by promoting iron uptake into the procaryote *Pseudomonas aeruginosa* [17]. In view of the similarities between Ins(1,2,3)P₃ and InsP₆ in their ability to inhibit HO· production, we examined whether Ins(1,2,3)P₃ also had siderophore activity. As can be seen in Fig. 4, Ins(1,2,3)P₃ promoted iron uptake with an activity comparable to that of InsP₆. Thus, in two different assays of Fe³⁺ binding, the two compounds resemble each other. We have observed increased transport of Fe³⁺ into *Pseudomonas aeruginosa* from inositol phosphates lacking a phosphate group at position 3, suggesting the rate by

Table 5

Inhibition by *myo*-inositol phosphates of HO·-mediated formaldehyde production

Inositol phosphate	Formaldehyde produced ^a (%)	
	10 μM phosphate	100 μM phosphate
(±)-Ins(1,2)P ₂	125 ± 4	225 ± 30
Ins(1,2,3)P ₃	51 ± 8	7 ± 2
(±)-Ins(1,2,3,4)P ₄	87 ± 4	9 ± 2
Ins(1,2,3,5)P ₄	67 ± 5	2 ± 0.3
(±)-Ins(1,2,4,5)P ₄	86 ± 7	66 ± 3
(±)-Ins(1,2,4,6)P ₄	91 ± 5	70 ± 2
(±)-Ins(1,2,5,6)P ₄	95 ± 5	77 ± 2
(±)-Ins(1,3,4,5)P ₄	95 ± 6	88 ± 7
Ins(1,3,4,6)P ₄	101 ± 4	85 ± 8
(±)-Ins(1,4,5,6)P ₄	97 ± 6	82 ± 5
Ins(2,4,5,6)P ₄	99 ± 5	78 ± 4
InsP ₆	53 ± 5	0

^a Values represent the amounts of formaldehyde produced, as percentages of control incubations without added inositol phosphates ($n = 4$).

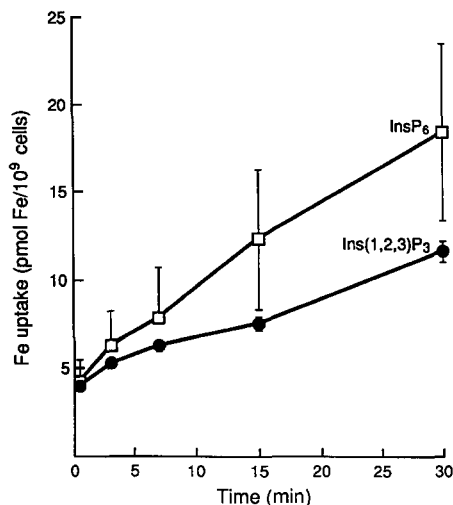


Fig. 4. ^{55}Fe transport from inositol phosphates into *Pseudomonas aeruginosa*. A 1:500 complex was formed by addition of 200 nM $^{55}\text{FeCl}_3$ to 100 μM inositol phosphate.

which Fe^{3+} crosses the cell envelope may be a function of the putative carrier system to remove iron from the inositol phosphate [47].

3. Experimental

General.—NMR spectra were recorded on a Bruker 250-AC spectrometer: ^1H (250.1 MHz), ^{31}P (101.3 MHz), and ^{13}C (62.9 MHz); or a Jeol EX-270 MHz spectrometer: ^1H (270.0 MHz), ^{31}P (109.2 MHz), and ^{13}C (67.8 MHz). The ^1H and ^{13}C NMR spectra were referenced to tetramethylsilane unless otherwise stated, and ^{31}P NMR spectra were referenced to 85% phosphoric acid. All ^{13}C and ^{31}P NMR spectra were ^1H decoupled unless otherwise stated. IR spectra were recorded on a Philips PU 9516 spectrometer or a FT-IR Mattson 2020 Galaxy Series instrument. Mass spectra were recorded on a Kratos Concept 1-S mass spectrometer, using xenon as a carrier gas and 3-nitrobenzyl alcohol as a matrix for FAB; a VG Micromass 12 instrument at 70 eV and a source temperature of 300 $^\circ\text{C}$; or a VG 7070E instrument, using positive ion FAB with a 3-nitrobenzyl alcohol matrix. Melting points were measured on a Kofler Reichert–Jung hot stage or a Gallenkamp digital capillary apparatus. Elemental analyses were measured at Butterworths Laboratories, Middlesex, or at the Micro Analytical Laboratory, Department of Chemistry, University of Manchester. Flash column chromatography [48] was performed using Sorbsil C60 40/60H silica gel. TLC was performed using Merck aluminium-backed Silica Gel 60 plates containing a fluorescent indicator. Spots were visualised under 254-nm UV light or with I_2 . The following solvents were purified by heating under reflux followed by distillation over the appropriate drying reagent: CH_2Cl_2 (P_2O_5), THF (Na–benzophenone), and toluene (Na). A preliminary account of the synthesis of all regioisomeric *myo*-inositol tetrakisphosphates has been reported [27] and further details will be published elsewhere.

(±)-*cis*-1,2-*O*-Cyclohexylidene-*myo*-inositol (**3**).—Acetal **3** was prepared by adapting the method described by Baker and co-workers [29]. A mixture of bis(cyclohexylidene) acetals of *myo*-inositol (74.3 g, 0.218 mol) (prepared from the reaction of 1,1-diethoxycyclohexane with inositol [29]) was dissolved in toluene (200 mL), hexane (200 mL), and ethanol (100 mL). *p*-Toluenesulphonic acid (2.4 g, 12.6 mmol) was added and the mixture was maintained at 4 °C for 2 h. Triethylamine (2.4 mL, 17.2 mmol) was added and the solution was stored at –20 °C for 24 h. Compound **3** (30.1 g, 53%) was isolated by filtration; mp 179–181 °C, lit. mp 181–183 °C [29].

(±)-1-*O*-(*tert*-Butyldiphenylsilyl)-2,3-*O*-cyclohexylidene-*myo*-inositol (**4**).—Compound **4** was prepared utilising the procedure developed by Bruzik and Tsai [30]. *tert*-Butyldiphenylsilyl chloride (5.1 mL, 19.4 mmol) was added to a stirred solution of **3** (5 g, 19.2 mmol) and imidazole (1.96 g, 28.8 mmol) in pyridine (70 mL) at –10 °C. After 24 h, the reaction mixture was concentrated in vacuo. The residue was dissolved in CH₂Cl₂ (100 mL), washed with H₂O (100 mL), 1 M NaHCO₃ (100 mL), and H₂O (100 mL), dried (MgSO₄), and concentrated in vacuo. Crystallisation from DMF–CHCl₃–hexane afforded **4** as colourless plate crystals (5.34 g, 57.6%), which were used for X-ray diffraction structure determination; mp 98–100 °C; ¹H NMR data (250.1 MHz, CDCl₃, assigned with the aid of a COSY spectrum and decoupling experiments): δ 1.09 (s, 9 H, *t*-Bu), 1.2–1.7 (m, 10 H, cyclohexylidene), 2.52 (d, 1 H, *J*_{H,OH} 2.3 Hz, OH), 2.74 (s, 1 H, OH), 2.90 (s, 1 H, OH), 3.12 (t, 1 H, *J*_{5,4} ≈ *J*_{5,6} ≈ 9.5 Hz, H-5), 3.55–3.75 (m, 3 H, H-1,3,4), 3.85–3.9 (m, 2 H, H-2,6), 7.3–7.5 (m, 6 H, Ph), 7.7–7.8 (m, 4 H, Ph); IR data (KBr): *v*_{max} 3600–3100 cm⁻¹ (OH); MS data (CI): observed accurate mass 499.2516 (M + H⁺), C₂₈H₃₉O₆Si requires 499.2516 (M + H⁺).

(±)-4,5,6-Tri-*O*-benzoyl-1-*O*-(*tert*-butyldiphenylsilyl)-2,3-*O*-cyclohexylidene-*myo*-inositol (**5**).—Benzoyl chloride (7.70 mL, 66.4 mmol) was added to a solution of **4** (3.54 g, 7.1 mmol) and 4-dimethylaminopyridine (DMAP) (0.43 g, 3.5 mmol) in pyridine (50 mL) at room temperature under Ar. The mixture was heated at reflux for 20 h and then concentrated in vacuo. The residue was diluted with CH₂Cl₂ (100 mL), washed with H₂O (100 mL), 1 M NaHCO₃ (100 mL), and H₂O (100 mL), dried (MgSO₄), and concentrated in vacuo. The crude product was subjected to flash chromatography on silica gel, eluting with 1:3 diethyl ether–hexane. Colourless plate crystals of **5**, suitable for X-ray crystallography, were isolated (4.23 g, 73.4%); mp 173.5–175 °C; ¹H NMR data (250.1 MHz, CDCl₃, assigned with the aid of a COSY spectrum and decoupling experiments): δ 0.95 (s, 9 H, *t*-Bu), 1.15–2.1 (m, 10 H, cyclohexylidene), 4.05–4.2 (m, 2 H, H-2,3), 4.30 (dd, 1 H, *J*_{1,2} 3.9, *J*_{1,6} 9.3 Hz, H-1), 5.36 (t, 1 H, *J*_{5,4} ≈ *J*_{5,6} ≈ 9.8 Hz, H-5), 5.79 (dd, 1 H, *J*_{4,5} 10.3, *J*_{4,3} 7.0 Hz, H-4), 6.03 (t, 1 H, *J*_{6,1} ≈ *J*_{6,5} ≈ 9.4 Hz, H-6), 7.1–7.9 (m, 25 H, Ph); ¹³C NMR data (62.9 MHz, CDCl₃): δ 19.0 (CMe₃), 23.8, 23.9, 24.9 (3 × CH₂ of cyclohexylidene), 26.5 (CMe₃), 34.7, 37.7 (2 × CH₂ of cyclohexylidene), 70.1, 71.1, 72.2, 73.7, 75.5, 75.6 (6 × inositol CH), 111.4 (C-1 of cyclohexylidene), 127.5, 127.6, 128.0, 128.1, 128.7, 129.3, 129.6, 129.7, 129.9, 132.3, 132.8, 132.9, 133.6, 135.9 (phenyl), 165.3, 165.4, 165.7 (3 × C=O); IR data (KBr): *v*_{max} 1735 cm⁻¹ (C=O); MS data (positive ion FAB): observed accurate mass 833.3103 (M + Na⁺), C₄₉H₅₀O₉SiNa requires 833.3122 (M + Na⁺). Anal. Calcd for C₄₉H₅₀O₉Si: C, 72.57; H, 6.21. Found C, 72.51; H, 6.13.

4,5,6-Tri-O-benzoyl-myo-inositol (6).—A solution of **5** (200 mg, 0.25 mmol) in 7:3 $\text{CF}_3\text{CO}_2\text{H-H}_2\text{O}$ (8 mL) was stirred at 50 °C for 2 days. The mixture was concentrated in vacuo, the residue diluted with diethyl ether (20 mL), and the solution washed with H_2O (3×20 mL), dried (MgSO_4), and concentrated in vacuo. A small amount of diethyl ether was added and **6** then precipitated overnight at 4 °C; **6** was further purified by precipitation from diethyl ether (59 mg, 49%); mp 100.5–103 °C; ^1H NMR data (250.1 MHz, CD_3OD , assignments made with the aid of a COSY spectrum): δ 4.02 (dd, 2 H, $J_{1,2}$ 2.7, $J_{1,6}$ 9.7 Hz, H-1), 4.19 (t, 1 H, $J_{2,1}$ 2.7 Hz, H-2), 5.67 (t, 1 H, $J_{5,4}$ 9.9 Hz, H-5), 5.85 (t, 2 H, $J_{4,5}$ 9.9 Hz, H-4), 7.2–7.5 (m, 9 H, Ph), 7.6–7.75 (m, 2 H, Ph), 7.9–7.95 (m, 4 H, Ph); ^1H NMR data (250.1 MHz, $\text{Me}_2\text{SO}-d_6$): δ 3.9–4.1 (m, 3 H, H-1,2), 5.27 (d, 2 H, $J_{1,\text{OH}}$ 6.1 Hz, HO-1, exchangeable with D_2O), 5.50 (d, 1 H, $J_{2,\text{OH}}$ 2.9 Hz, HO-2, exchangeable with D_2O), 5.6–5.8 (m, 3 H, H-4,5), 7.3–7.9 (m, 15 H, Ph); ^{13}C NMR data (62.9 MHz, $\text{Me}_2\text{SO}-d_6$): δ 69.1 ($2 \times \text{C}$), 72.8, 73.1, 73.7 ($2 \times \text{C}$) (inositol CH), 128.8, 128.9, 129.1, 129.3, 129.9, 133.5, 133.6 (phenyl), 165.3 (C=O), 165.6 ($2 \times \text{C}=\text{O}$); IR data (KBr): ν_{max} 3475 (OH), 3415 (OH), 1727 (C=O) cm^{-1} ; MS data (CI): observed accurate mass 493.1499 ($\text{M} + \text{H}^+$), $\text{C}_{27}\text{H}_{25}\text{O}_9$ requires 493.1499 ($\text{M} + \text{H}^+$). Anal. Calcd for $\text{C}_{27}\text{H}_{24}\text{O}_9 \cdot 0.5\text{H}_2\text{O}$: C, 64.67; H, 5.02. Found C, 64.52; H, 4.74.

4,5,6-Tri-O-benzoyl-myo-inositol 1,2,3-tris(dibenzyl phosphate) (7).—Dibenzyl *N,N*-diisopropylphosphoramidite [32] (1.69 g, 4.87 mmol) was added to a solution of **6** (0.40 g, 0.81 mmol) and 1*H*-tetrazole (0.68 g, 9.76 mmol) in CH_2Cl_2 (40 mL). The mixture was stirred under Ar at room temperature for 2 h to give the trisphosphite; ^{31}P NMR data (101.3 MHz, CDCl_3): δ 140.9 (s, 2 P), 139.9 (s, P). The reaction mixture was cooled to –40 °C and a solution of 3-chloroperoxybenzoic acid (1.4 g, ~6.5 mmol) in CH_2Cl_2 (40 mL) was added. The mixture was stirred at 0 °C for 1 h after which time the solution was concentrated in vacuo. Crystallisation from diethyl ether–hexane afforded **7** (0.57 g, 55.5%) as colourless laths; the crystals were solved by X-ray diffraction and shown to contain one molecule of water per formula unit [1]; mp 131.5–132.5 °C; ^1H NMR data (250.1 MHz, CDCl_3 , assignments were made with the aid of a COSY spectrum): δ 4.45 (dd, 2 H, J_{gem} 11.7, $J_{\text{P,H}}$ 8.9 Hz, $2 \times \text{P-O-CH}_A\text{H}_B\text{Ph}$), 4.66 (dd, 2 H, J_{gem} 11.8, $J_{\text{P,H}}$ 7.5 Hz, $2 \times \text{P-O-CH}_A\text{H}_B\text{Ph}$), 4.9–5.05 (m, 6 H, $2 \times \text{P-O-CH}_2\text{Ph}$, H-1), 5.22 (d, 4 H, $J_{\text{P,H}}$ 6.1 Hz, $2 \times \text{P-O-CH}_2\text{Ph}$), 5.56 (br d, 1 H, $J_{\text{P,H}}$ 9.3 Hz, H-2), 5.75 (t, 1 H, $J_{5,4}$ 10.0 Hz, H-5), 6.16 (t, 2 H, $J_{4,3} \approx J_{4,5} \approx 10.1$ Hz, H-4), 6.81 (d, 4 H, $J_{\text{H,H}}$ 7.1 Hz, Ph), 7.05–7.5 (m, 35 H, Ph), 7.79 (d, 2 H, $J_{\text{H,H}}$ 7.3 Hz, Ph), 7.91 (d, 4 H, $J_{\text{H,H}}$ 7.3 Hz, Ph); ^{13}C NMR data (62.9 MHz, CDCl_3 , assignments made with the aid of a DEPT spectrum): δ 69.5 (d, $J_{\text{P,C}}$ 5.7 Hz, $2 \times \text{PhCH}_2\text{OP}$), 69.65 (d, $J_{\text{P,C}}$ 5.3 Hz, $2 \times \text{PhCH}_2\text{OP}$), 69.85 (d, $J_{\text{P,C}}$ 6.2 Hz, $2 \times \text{PhCH}_2\text{OP}$), 70.0 (d, $J_{\text{P,C}}$ 3.8 Hz, $2 \times$ inositol CH), 70.3 (s, inositol CH), 73.8 (br s, $2 \times$ inositol CH), 77.1 (br s, inositol CH), 127.5, 128.0, 128.05, 128.2, 128.3, 128.35, 128.45, 129.7, 129.9, 133.25 (all s, aromatic CH), 128.8 [s, $3 \times$ quat. $\text{PhC}(\text{O})$], 135.0 (d, $J_{\text{P,C}}$ 6.7 Hz, $2 \times$ quat. PhCH_2OP), 135.4 (d, $J_{\text{P,C}}$ 8.6 Hz, $2 \times$ quat. PhCH_2OP), 135.6 (d, $J_{\text{P,C}}$ 8.6 Hz, $2 \times$ quat. PhCH_2OP), 165.3 (s, C=O), 165.4 (s, $2 \times \text{C}=\text{O}$); ^{31}P NMR data (101.3 MHz, CDCl_3): δ –1.06 (s, P-1,3), –2.22 (s, P-2); ^{31}P NMR data (101.3 MHz, CDCl_3 , ^1H coupled): δ –1.18 (sextet, $J_{\text{P,H}}$ 8.3 Hz), –2.30 (br sextet, $J_{\text{P,H}}$ ~6.8 Hz); IR data (KBr): ν_{max} 1269 (P=O), 1733 (C=O) cm^{-1} ; MS data (positive ion FAB): observed

accurate mass 1273.3311 ($M + H^+$), $C_{69}H_{64}P_3O_{18}$ requires 1273.3306 ($M + H^+$). Anal. Calcd for $C_{69}H_{63}P_3O_{18} \pm H_2O$: C, 64.19; H, 5.07. Found: C, 63.82; H, 4.89.

Monosodium tetra(cyclohexylammonium) salt of myo-inositol 1,2,3-trisphosphate (1).—A solution of **7** (130 mg, 0.102 mmol) and Pd–C catalyst (10%, 30 mg) in EtOH (20 mL) was stirred under H_2 for 24 h at room temperature. The catalyst was removed by filtration through Celite to give the free acid; ^{31}P NMR data (101.3 MHz, CD_3OD): δ 1.80 (s, 1 P), 1.43 (s, 2 P). The reaction mixture was concentrated under vacuum and the residue was treated with 0.5 M NaOH (20 mL) for 12 h at room temperature. The solution was applied to a column of cation-exchange resin (Dowex 50-X8, mesh 20–50, 20 mL, H^+ form), which was eluted with water (60 mL)³. Benzoic acid was removed by extraction into $CHCl_3$ and the pH of the aqueous layer was adjusted to 11 with cyclohexylamine. The solution was concentrated under vacuum, the residue was redissolved in water (2 mL), and acetone was added to crystallise **1** as its dihydrated monosodium tetra(cyclohexylammonium) salt (73 mg, 82%) as confirmed by X-ray crystallography [33]⁴; mp 165–166.5 °C; 1H NMR data (250.1 MHz, D_2O , referenced to acetone at 2.22 ppm): δ [1.1–1.45 (m, 20 H), 1.64 (br d, 4 H, $J_{H,H}$ 11.9 Hz), 1.79 (br d, 8 H, $J_{H,H}$ 3.8 Hz), 1.97 (br s, 8 H), 3.0–3.25 (m, 4 H), 4 \times cyclohexylammonium], 3.39 (t, 1 H, $J_{4,5}$ 9.2 Hz, H-5), 3.83 (t, 2 H, $J_{4,3} \approx J_{4,5} \approx 9.5$ Hz, H-4), 3.98 (br t, 2 H, $J_{1,6} \approx J_{P,H} \approx 8.9$ Hz, H-1), 4.72 (br d, 1 H, $J_{P,H}$ 9.8 Hz, H-2); ^{13}C NMR data (62.9 MHz, D_2O , referenced to Me_2SO-d_6 at 39.7 ppm): δ 23.1, 23.6, 29.7 (all s, ratios 2:1:2, CH_2 of cyclohexylammonium), 49.5 (CH of cyclohexylammonium), 71.2 (d, $J_{P,C}$ 3.8 Hz, 2 \times inositol CH), 73.2 (br s, 2 \times inositol CH), 73.7 (s, inositol CH), 74.3 (br s, inositol CH); ^{31}P NMR data (101.3 MHz, D_2O): δ 1.70 (s, P-2), 3.62 (s, P-1,3); ^{31}P NMR data (101.3 MHz, D_2O , 1H coupled): δ 1.70 (d, $J_{P,H}$ 8.5 Hz), 3.62 (d, $J_{P,H}$ 6.1 Hz); MS data (positive ion FAB): 421 (38%, $C_6H_{16}O_{15}P_3$, free acid + H), 443 (100%, $C_6H_{15}O_{15}P_3Na$, free acid + Na), 465 (22%, $C_6H_{14}O_{15}P_3Na_2$, free acid + 2Na – H), 520 (25%, free acid + cyclohexylammonium). Anal. Calcd for $C_{30}H_{66}N_4O_{15}P_3Na \cdot 2H_2O$: C, 41.19; H, 8.06; N, 6.40. Found: C, 41.42; H, 8.41; N, 6.42.

(\pm)-3,4,5,6-Tetra-*O*-benzyl-myoinositol 1,2-bis(dibenzyl phosphate) (**9**).—A solution of (\pm)-3,4,5,6-tetra-*O*-benzyl-myoinositol (**8**) [29] (500 mg, 0.926 mmol), 1*H*-tetrazole (389 mg, 5.56 mmol), and dibenzyl *N,N*-diisopropylphosphoramidite [32] (1.28 g, 3.70 mmol) in CH_2Cl_2 (40 mL) was stirred for 90 min at room temperature under N_2 . The mixture was cooled to $-78^\circ C$ and a solution of 3-chloroperoxybenzoic acid (1.12 g, 57–86%, > 3.70 mmol) in CH_2Cl_2 (15 mL) was added dropwise. After 30 min, the solution was allowed to warm up to room temperature over 30 min, and then washed successively with aqueous $NaHSO_3$ (10% w/v, 2 \times 20 mL), saturated aqueous $NaHCO_3$ (2 \times 20 mL), and water (20 mL). The organic layer was dried ($MgSO_4$) and the solvent was removed under vacuum. The residue was purified by flash column chromatography

³ Extrapolating back from the X-ray crystal structure and elemental analysis data of the final product suggests that the monosodium salt of myo-inositol 1,2,3-trisphosphate is present at this stage, presumably attributable to the low pK_a of the first ionisation: for phytic acid this pK_a (at C-2) is 1.1 [49].

⁴ The monosodium tetra(cyclohexylammonium) salt of **1** is formed, presumably due to the very high sixth pK_a value: for phytic acid the highest pK_a value (at C-3) is 12.0 [49], and the pK_a of cyclohexylamine is 10.64 [50]. The highest pK_a value for myo-inositol 1,2,3-trisphosphate has been measured as 9.56 [51].

on silica gel, eluting with 45:55 EtOAc–hexane to give **9** as a colourless oil (961 mg, 98%); ^1H NMR data (270.0 MHz, CDCl_3 , assignments made with the aid of a COSY spectrum): δ 3.45–3.55 (m, 1 H, H-3), 3.52 (t, 1 H, $J_{5,4} \approx J_{5,6} \approx 9.2$ Hz, H-5), 3.87 (t, 1 H, $J_{4,5} \approx J_{4,3} \approx 9.7$ Hz, H-4), 3.95 (t, 1 H, $J_{6,5} \approx J_{6,1} \approx 9.7$ Hz, H-6), 4.40 (tt, 1 H, $J_{\text{P,H}} \approx J_{1,6} \approx 9.6$ Hz, $J_{1,2} \approx J_{\text{P,H}} \approx 2.3$ Hz, H-1), 4.49 (d, 1 H, J_{gem} 10.9 Hz, C–O–CH–HPh), 4.64 (d, 1 H, J_{gem} 11.9 Hz, C–O–CHHPh), 4.7–5.05 (m, 10 H, $5 \times \text{CH}_2\text{Ph}$), 5.08 (dd, 4 H, J_{gem} 11.7, $J_{\text{P,H}}$ 7.1 Hz, P–O–CHHPh), 5.39 (dt, 1 H, $J_{\text{P,H}}$ 8.6, $J_{2,1} \approx J_{2,3} \approx 2.3$ Hz, H-2), 7.1–7.4 (m, 40 H, $8 \times \text{Ph}$); ^{13}C NMR data (67.8 MHz, CDCl_3): δ 69.15 (d, $J_{\text{P,C}}$ 6.1 Hz, $2 \times \text{PhCH}_2\text{OP}$), 69.4 (d, $J_{\text{P,C}}$ 4.8 Hz, PhCH_2OP), 69.5 (d, $J_{\text{P,C}}$ 3.7 Hz, PhCH_2OP), 72.65 (s, PhCH_2OC), 75.5 (s, PhCH_2OC), 75.6 (d, $J_{\text{P,C}}$ 7.3 Hz, inositol CH), 75.9 (s, PhCH_2OC), 76.1 (s, PhCH_2OC), 76.5 (s, inositol CH, beneath the upfield signal of CDCl_3 triplet), 78.5 (s, inositol CH), 79.55 (d, $J_{\text{P,C}}$ 4.9 Hz, inositol CH), 80.65 (s, inositol CH), 82.65 (s, inositol CH), 127.3–128.6 (14 singlets for 40 aromatic CH), 135.65 (d, $J_{\text{P,C}}$ 7.4 Hz, quat. PhCH_2OP), 135.85 (d, $J_{\text{P,C}}$ 7.3 Hz, quat. PhCH_2OP), 135.95 (d, $J_{\text{P,C}}$ 6.1 Hz, quat. PhCH_2OP), 136.0 (d, $J_{\text{P,C}}$ ~ 8 Hz, quat. PhCH_2OP), 137.3 (s, quat. PhCH_2OC), 138.1 (s, quat. PhCH_2OC), 138.15 (s, quat. PhCH_2OC), 138.3 (s, quat. PhCH_2OC); ^{31}P NMR data (109.2 MHz, CDCl_3): δ -2.00, -0.97; IR data (thin film): ν_{max} 1280 cm^{-1} (P=O); MS data (positive ion FAB): 1061 (M + H, 83%), 1060 (100%). Anal. Calcd for $\text{C}_{62}\text{H}_{62}\text{O}_{12}\text{P}_2$: C, 70.18; H, 5.89. Found: C, 70.25; H, 6.04.

Trisodium (\pm)-myo-inositol 1,2-bisphosphate (2).—A solution of **9** (138 mg, 0.13 mmol) in THF (7 mL) and water (7 mL) was stirred with Pd–C catalyst (10%, 200 mg) under H_2 for 18 h at room temperature. The catalyst was removed by filtration through Celite and the filtrate was concentrated under vacuum without heating. The residue was dissolved in water (5 mL) and applied to a column of cation-exchange resin (Dowex 50-X8, mesh 20–50, 50 mL, Na^+ form) which was eluted with water (150 mL). The water was evaporated under vacuum to give **2** as a colourless solid (48 mg, 87%); mp > 300 $^\circ\text{C}$; ^1H NMR data (270.0 MHz, D_2O , referenced to benzene at 7.44 ppm, assignments were made with the aid of a COSY spectrum): δ 3.33 (t, 1 H, $J_{5,4} \approx J_{5,6} \approx 9.2$ Hz, H-5), 3.50 (d, 1 H, $J_{3,4}$ 9.9 Hz, H-3), 3.74 (t, 1 H, $J_{4,3} \approx J_{4,5} \approx 9.6$ Hz, H-4), 3.83 (t, 1 H, $J_{6,1} \approx J_{6,5} \approx 9.6$ Hz, H-6), 3.98 (t, 1 H, $J_{\text{P,H}} \approx J_{1,6} \approx 7.9$ Hz, H-1), 4.71 (d, 1 H, $J_{\text{P,H}}$ 8.6 Hz, H-2); ^{13}C NMR data (67.8 MHz, D_2O , referenced to benzene at 128.5 ppm): δ 71.4 (s), 72.1 (d, $J_{\text{P,C}}$ 6.1 Hz), 73.0 (s), 74.2 (s), 74.35 (t, $J_{\text{P,C}}$ 5.5 Hz), 74.5 (d, $J_{\text{P,C}}$ 4.9 Hz); ^{31}P NMR data (109.2 MHz, D_2O): δ 1.02, 3.33. Anal. Calcd for $\text{C}_6\text{H}_{10}\text{O}_{12}\text{P}_2\text{Na}_4$: C, 16.84; H, 2.35. Calcd for $\text{C}_6\text{H}_{11}\text{O}_{12}\text{P}_2\text{Na}_3 \cdot \text{H}_2\text{O}$: C, 16.99; H, 3.09. Found: C, 17.17; H, 3.00 (dried). Calcd for $\text{C}_6\text{H}_{11}\text{O}_{12}\text{P}_2\text{Na}_3 \cdot 3.5\text{H}_2\text{O}$: C, 15.36; H, 3.87; P, 13.21; Na, 14.70. Found: C, 15.78; H, 4.02; P, 12.52; Na, 14.43 (hydrate).

Crystal structure determination.—Crystal data for compounds **4** and **5** were measured using an Enraf–Nonius CAD4-F 4-circle diffractometer with graphite-monochromated Mo- K_α X-ray radiation ($\gamma = 0.71069$ \AA). The space group was determined unambiguously as a result of structure analysis. The unit cell parameters were obtained by least-squares refinement, the setting angles of 25 accurately centred reflections being used for this purpose. Reflected intensities were collected by the ω – 2θ scan technique for **4** and **5** out to Bragg angles θ of 24 and 25 $^\circ$, respectively. The ω scan angle was calculated from $[M + N(\tan \theta)]^\circ$, where $M = 0.9$, $N = 0.35$, and increased by 25% on

each side for background determination. The scan speed was varied from 0.6 to 2.1 and 0.5 to 1.8° min⁻¹ depending upon the intensity for **4** and **5**, respectively. Three standard reflections were measured every hour during data collection and showed no appreciable variation with time. The data were corrected for Lorentz and polarisation effects. The structures were solved by direct methods using MULTAN 84 [52] and refined by the full-matrix least-squares method on F^2 for all data using SHELXL-93 [53] which included parameters for atomic coordinates, temperature factors (anisotropic for non-hydrogen atoms), an overall scale factor, and an extinction parameter. Reflections for **4** and **5** were weighted according to $1/[\sigma^2(F_o^2) + (0.1000P)^2 + 0.0000P]$ where $P = (F_o^2 + 2F_c^2)/3$. From difference electron density maps, hydrogen positions for **4** and **5** were found on the inositol rings and on the OH groups for **4**. The other hydrogen atoms were assumed to ride on attached atoms and were placed in calculated positions since they were not found on the difference map. Common temperature factors for hydrogen atoms in chemical groups of similar kind were set as free variables. Final difference Fourier series showed no significant residual electron density and there were no exceptional discrepancies between observed and calculated structure factors.

Hydroxyl radical generation.—HO· generation was measured as described previously [16], except that it was not necessary to add H₂O₂.

Iron uptake into Pseudomonas aeruginosa.—Experiments were performed as described previously [17].

Acknowledgements

We thank Dr. J. Godward for recording some of the NMR spectra, Drs. P.T. Hawkins and R.F. Irvine for helpful discussions, BBSRC for a studentship (IDS), the Lister Institute for a fellowship (SF), and the University of Manchester Research Support Fund (KS). The research at Pohang University was supported by the Korea Science and Engineering Foundation and the Ministry of Education. The mass spectra were recorded at the EPSRC mass spectrometry service (University of Swansea) or at the Department of Chemistry, University of Manchester.

References

- [1] I.D. Spiers, S. Freeman, D.R. Poyner, and C.H. Schwalbe, *Tetrahedron Lett.*, 36 (1995) 2125–2128.
- [2] D.J. Cosgrove, *Inositol Phosphates, their Chemistry, Biochemistry and Physiology*, Elsevier, Amsterdam, 1980.
- [3] A.M. Shamsuddin, *J. Nutr.*, 125 (1995) 725S–732S.
- [4] F.S. Menniti, K.G. Oliver, J.W. Putney, and S.B. Shears, *TIBS*, 18 (1993) 53–56.
- [5] L. Stephens, T. Radenberg, U. Thiel, G. Vogel, K.-H. Khoo, A. Dell, T.R. Jackson, P.T. Hawkins, and G.W. Mayr, *J. Biol. Chem.*, 268 (1993) 4009–4015.
- [6] M. Vallejo, T. Jackson, S. Lightman, and M.R. Hanley, *Nature (London)*, 330 (1987) 656–658.
- [7] M.-K. Sun, C. Wahlestedt, and D.J. Reis, *Eur. J. Pharmacol.*, 215 (1992) 9–16.
- [8] E. Graf and J.W. Eaton, *Free Radical Biol. Med.*, 8 (1990) 61–69.
- [9] E. Graf, J.R. Mahoney, R.G. Bryant, and J.W. Eaton, *J. Biol. Chem.*, 259 (1984) 3620–3624.
- [10] B. Halliwell and J.M.C. Gutteridge, *Free Radicals in Biology and Medicine*, 2nd ed., Clarendon Press, Oxford, 1989.

- [11] E. Graf, K.L. Empson, and J.W. Eaton, *J. Biol. Chem.*, 262 (1987) 11647–11650.
- [12] M.J. Burkitt and B.C. Gilbert, *Free Radical Res. Commun.*, 10 (1990) 265–280.
- [13] M.J. Burkitt and B.C. Gilbert, *Free Radical Res. Commun.*, 14 (1991) 107–123.
- [14] R.A. Floyd and C.A. Lewis, *Biochemistry*, 22 (1983) 2645–2649.
- [15] D.R. Poyner, F. Cooke, M.R. Hanley, D.J.M. Reynolds, and P.T. Hawkins, *J. Biol. Chem.*, 268 (1993) 1032–1038, and references therein.
- [16] P.T. Hawkins, D.R. Poyner, T.R. Jackson, A.J. Letcher, D.A. Lander, and R.F. Irvine, *Biochem. J.*, 294 (1993) 929–934.
- [17] A.W. Smith, D.R. Poyner, H.K. Hughes, and P.A. Lambert, *J. Bacteriol.*, 176 (1994) 3455–3459.
- [18] G.E. Blank, J. Pletcher, and M. Sax, *Acta Crystallogr., Sect. B*, 31 (1975) 2584–2592.
- [19] A. Arnone and M.F. Perutz, *Nature (London)*, 249 (1974) 34–36.
- [20] L.R. Isbrandt and R.P. Oertel, *J. Am. Chem. Soc.*, 102 (1980) 3144–3148.
- [21] W.J. Evans and C.J. Martin, *J. Inorg. Biochem.*, 34 (1988) 11–18.
- [22] W.J. Evans and C.J. Martin, *J. Inorg. Biochem.*, 41 (1991) 245–252.
- [23] F.M. McConnell, S.B. Shears, P.J.L. Lane, M.S. Scheibel, and E.A. Clark, *Biochem. J.*, 284 (1992) 447–455.
- [24] C.J. Barker, P.J. French, A.J. Moore, T. Nilsson, P.-O. Berggren, C.M. Bunce, C.J. Kirk, and R.H. Michell, *Biochem. J.*, 306 (1995) 557–564.
- [25] C.J. Barker, J. Wright, C.J. Kirk, and R.H. Michell, *Biochem. Soc. Trans.*, 23 (1995) 169S.
- [26] D.C. Billington, *The Inositol Phosphates. Chemical Synthesis and Biological Significance*, VCH, Weinheim, 1993, p 53.
- [27] S.-K. Chung and Y.-T. Chang, *J. Chem. Soc., Chem. Commun.*, (1995) 11–12.
- [28] C.E. Dreef, R.J. Tushman, A.W.M. Lefebvre, C.J.J. Elle, G.A. van der Marel, and J.H. van Boom, *Tetrahedron*, 47 (1991) 4709–4722.
- [29] G.R. Baker, D.C. Billington, and D. Gani, *Tetrahedron*, 47 (1991) 3895–3908.
- [30] K.S. Bruzik and M.-D. Tsai, *J. Am. Chem. Soc.*, 114 (1992) 6361–6374.
- [31] S.-K. Chung and Y.-T. Chang, *J. Chem. Soc., Chem. Commun.*, (1995) 13–14.
- [32] K.-L. Yu and B. Fraser-Reid, *Tetrahedron Lett.*, 29 (1988) 979–982.
- [33] I.D. Spiers, S. Freeman, and C.H. Schwalbe, *J. Chem. Soc., Chem. Commun.*, (1995) 2219–2220.
- [34] H.D. Flack, *Acta Crystallogr., Sect. A*, 39 (1983) 876–881.
- [35] I.N. Rabinowitz and J. Kraut, *Acta. Crystallogr.*, 17 (1964) 159–168.
- [36] C.K. Johnson, ORTEP, Report ORNL-5136, Oak Ridge National Laboratory, TN, USA, 1976.
- [37] W.L. Duax and D.A. Norton, *Atlas of Steroid Structure*, Plenum, New York, 1975, pp 16–22.
- [38] T. Steiner and W. Saenger, *Acta. Crystallogr., Sect. B*, 48 (1992) 819–827.
- [39] G.A. Jeffrey and W. Saenger, *Hydrogen Bonding in Biological Structures*, Springer, Berlin, 1991, p 333.
- [40] K.A. Abboud, S.H. Simonsen, R.J. Voll, and E.S. Youmathan, *Acta. Crystallogr., Sect. C*, 46 (1990) 2208–2210.
- [41] P. Deslongchamps, *Stereoelectronic Effects in Organic Chemistry*, Pergamon, Oxford, 1983.
- [42] S.M. Klein, G. Cohen, and A.I. Cederbaum, *Biochemistry*, 20 (1981) 6006–6012.
- [43] T. Nash, *Biochem. J.*, 55 (1953) 416–421.
- [44] B. Halliwell, *FEBS Lett.*, 92 (1978) 321–326.
- [45] K. Mernissi-Arifi, C. Wehrer, G. Schlewer, and B. Spiess, *J. Inorg. Biochem.*, 55 (1994) 263–277.
- [46] D.R. Poyner, unpublished results.
- [47] P.H. Hirst and A.W. Smith, unpublished results.
- [48] W.C. Still, M. Kahn, and A. Mitra, *J. Org. Chem.*, 43 (1978) 2923–2925.
- [49] A.J.R. Costello, T. Glonek, and T.C. Myers, *Carbohydr. Res.*, 46 (1976) 159–171.
- [50] A.M. James and M.P. Lord, *Macmillan's Chemical and Physical Data*, Macmillan, New York, 1992.
- [51] L. Schmitt, Ph.D. Thesis, Université Louis Pasteur de Strasbourg, France, 1993.
- [52] P. Main, G. Germain, and M.M. Woolfson, MULTAN 84, A System of Computer Programs for the Automatic Solution of Crystal Structures from X-Ray Diffraction Data, Universities of York, England and Louvain, Belgium, 1984.
- [53] G.M. Sheldrick, SHELXL-93, Program for Crystal Structure Refinement, University of Göttingen, Germany.